Axial dispersion of the liquid phase in a three-phase Karr reciprocating plate column

LJUBIŠA B. NIKOLIĆ[1*], VESNA D. NIKOLIĆ[1#], VLADA B. VELJKOVIĆ[1#], MIODRAG L. LAZIĆ[1] and DEJAN U. SKALA[2]

[1]*Faculty of Technology, Bulevar oslobođenja 124, 16000 Leskovac and* [2]*Faculty of Technology and Metallurgy, Karnegijeva 4, 11000 Belgrade, Serbia and Montenegro*

Abstract: The influence of the gas flow rate and vibration intensity in the presence of the solid phase (polypropylene spheres) on axial mixing of the liquid phase in a three phase (gas-liquid-solid) Karr reciprocating plate column (RPC) was investigated. Assuming that the dispersion model of liquid flow could be used for the real situation inside the column, the dispersion coefficient of the liquid phase was determined as a function of different operating parameters. For a two-phase liquid-solid RPC the following correlation was derived:

$$D_L = 1.26(Af)^{1.42} U_L^{0.51} \varepsilon_S^{0.23}$$

and a similar equation could be applied with ± 30 % confidence for the calculation of axial dispersion in the case of a three-phase RPC:

$$D_L = 1.39(Af)^{0.47} U_L^{0.42} U_G^{0.03} \varepsilon_S^{-0.26}$$

Keywords: Karr reciprocating plate column, three-phase column, axial dispersion, residence time distribution, dispersion model.

INTRODUCTION

Multiphase systems are very often applied in biotechnology (immobilized microbes or enzymes on a solid support used as a catalyst for microbic or enzyme fermentations) and chemical processes where the reactants and catalyst are present in different phases (gas–liquid and solid–catalyst). The reaction rate of such processes usually depends on the specific contact area between the phases (fluid and solid) as well as on the mass transfer rate from one phase to the other. External mixing in a reactor of different and specific construction and usage could generate phase dispersion.

The flow of phases in continuous processes is usually not ideal and in some cases such deviation from the ideal flow pattern (plug flow or ideal mixing) might be substantial. Such deviations from the ideal type of fluid flow are usually: channelling, recycle flow or stagnant zone formation inside the reactor or some other type of equipment used in the

---

*   To whom all correspondence should be addressed.

\#   Serbian Chemical Society active member.

chemical process industry (distillation columns, absorbers, adsorbers, heat exchanger). When such non-ideal behavior of fluid flow occurs, an important decrease of process unit productivity may be detected.

Knowing the effect of non-ideal flow is of particular importance in the case of scale-up design. In many cases it is enough to have information about the residence time distribution of a fluid in a reactor determined by stimulus-response methods with the appropriate tracer. The diminishing effects of non-ideal flow in the design of industrial units might lead to enormous errors in their exploitation.

Reciprocating plate columns (RPC) have primarily been used in the last few decades in the process of liquid-liquid extraction.[1,2] This type of unit must have good characteristics leading to small axial mixing of both the continuous and dispersed phases. The investigation presented in this paper was performed on a RPC of the Karr type, patented in 1959, characterized by a larger open area of the plates of the vibration set (< 60 %).[2] This type of column is known today as the Karr type of RPC. In industrial applications one may find columns with diameter up to 1.7 m and 18.3 m in height.[3]

This type of RPC has been used in the last two decades as a specific type of bioreactor.[4–8] The advantage of such a bioreactor compared to a bubble column is the evidence that external mixing generated by the vibration set increases the gas hold-up specific interfacial gas-liquid area in the column, thus improving the contact of phases. Finally, as a consequence of such a positive influence of vibrational mixing, one might calculate a substantial increase of the mass transfer rate between the phases. The uniformity of the phases in the radial direction (RPC columns of larger diameter) is also expressed, without channelling and dead zone effects or recycle flow. The relatively small external power consumption used for mixing the column content enables good mixing and phase dispersion, especially in the case of immiscible phases (aqueous and organic).

If laminar flow does not exist, the main problem in defining the mathematical model of a real reactor is how to define the fluid velocity profile. In such cases the dispersion model based on the assumption of the empirical parameter (dispersion coefficient) in the model equation is very often used. The mixing effect (in the axial and radial directions) is determined by a mathematical expression taking into account the effect of phase dispersion (dispersion model), which is determined by the effect of molecular diffusion. The residence time distribution function (F – function) and its density (function $E = \mathrm{d}F/\mathrm{d}t$) can be used for determining the coefficient of axial mixing (model parameter) based on the calculation of the central[9]:

$$\mu'_k = \int_0^\infty t^k E_t \, \mathrm{d}t \qquad \text{where } k = 0, 1, 2, 3, \dots \qquad (1)$$

and non-central moments of the E–function:

$$\mu'_k = \int_0^\infty (t - \mu_1)^k E_t \, \mathrm{d}t \qquad \text{where } k = 1, 2, 3, \dots \qquad (2)$$

The first non-central moment represents the average value of the E–function or the mean residence time of the fluid in the reactor (column), while the second central moments represent the dispersion of the residence time (σ_t^2).

By applying Eqs. 1 and 2, one can calculate the moments of the specific type of dispersion model (Table I).[9]

TABLE I. Values of dispersion coefficients, which can be calculated from the moments of the dispersion models (different type of broundary conditions; closed – dispersion does not exist; open – dispersion exists)

Model type (Inlet–Outlet)	The first non-central moment (The mean residence time)	Second central moment (Dispersion of the residence time)
Open–Open	$1 + 2/Pe$	$(2Pe+8)/Pe^2$
Open–Closed } Closed–Open }	$1 + 1/Pe$	$(2Pe+3)/Pe^2$
Closed–Closed	1	$\{2Pe–2[1–e^{-Pe}]\}/Pe^2$

The axial dispersion coefficient of the liquid phase in a multiphase RPC column (D_L) is determined on the basis of the calculated Pe number (Peclet) according to the equation:

$$D_L = \frac{U_L L}{Pe\,(1 - \varepsilon_G)(1 - \varepsilon_S)} \tag{3}$$

Different mathematical correlations derived for the calculation of axial dispersion in a RPC are given in Tables II–VI in the case of one (L–liquid), and two phase flow (G–L; gas–liquid and L–L systems), as well as in the case of bubble and packed-bed columns.

TABLE II. The axial dispersion coefficient in a RPC (correlations in the case of a one L–system)

System and operating parameters	Correlation	Reference
Water ↑; $D_c = 5$ cm; $f = 0.4 - 10$ Hz; $A = 0.15 - 0.45$ cm; $U_L = 0.3 - 0.5$ cm/s.	$D_L = 0.3\dfrac{h - 2m_1}{h - 4,5}\dfrac{2Afd^2}{\varepsilon}$ Where $2\,m_1 = \begin{cases} 105\left(\dfrac{2Af}{\varepsilon^2}\right)^{0.29} & \text{for } 2m_1 < 0.65(h+2.35) \\ 0.65(h+2.35) & \text{for other values} \end{cases}$	Nemecek and Prochazka (1974)[10]
Water, HCl solution, glucose or Polyox ↓; $D_c = 5.08$ cm; $f = 0.5 - 6$ Hz; $A < 2.35$ cm; $U_L = 0 - 1.2$ cm/s	$D_L = 1.98A^{1.74}f^{0.96}h^{-0.69}$ for teflon plates $D_L = 5.56A^{1.77}f^{1.00}h^{-1.32}$ for SS plates	Kim and Baird (1976)[11]
Solution of HCl ↓; $D_c = 5.08$ cm; $f = 0.5 - 6$ Hz; $A < 2.35$ cm; $U_L = 0 - 1.2$ cm/s; water ↓; $D_c = 2.54$ cm; $f = 0 - 10$ Hz; $A = 0 - 1.4$ cm; $U_L = 0.1 - 1.1$ cm/s.	$D_L \propto A^{1.80}f^{1.00}d^{1.8}\delta^{-0.3}h^{-1.3}$; $\ln D_L = \ln(D_L)_{f=0} + (Af)^{0.56}\exp(-1.44\,U_c + 0.912)$; where: $(D_L)_{f=0} = 5.15\,U_L^{0.471}$	Kim and Baird (1976)[12] Skala (1976)[13]
Water ↓; $D_c = 5.08$ cm; $f = 2.2 - 3.8$ Hz; $A = 1 - 1.85$ cm; $U_L = 0.5 - 1.32$ cm/s.	$D_L = \left\{ \dfrac{\ln\left(\dfrac{1+q}{q}\right)}{hU_c} + \dfrac{2\varepsilon\left(1 - \dfrac{K_2 A}{h}\right)}{K_1 d\left(U_c + 2\pi Af\right)\left[\left(\dfrac{\pi}{2\sqrt{3\varepsilon}}\right)^{0.5} - 1\right]} \right\}^{-1}$ K_1 and K_2 – dimensionless constants	Stevens and Baird (1990)[14]
Water ↑; $D_c = 5.08$ cm; $f = 0 - 5$ Hz; $A = 1.8 - 2.9$ cm; $U_L = 0.15 - 0.3$ cm/s.	$D_L = [l_m + (l_b - l_m)(\varepsilon_b/\varepsilon_t)^{0.34}]^{4/3}\varepsilon_t^{1/3}$; $l_m = 0.301$ cm; $l_b = 4.02$ cm	Baird and Rama Rao (1991)[15];
Water ↓; $D_c = 5$ cm; $f = 20 - 100$ Hz; $A < 0.012$ cm; $U_L = 0.23 - 0.44$ cm/s.	$\dfrac{D_L}{h\,U_L} = 0.5 + \alpha$	Baird et al. (1992)[16]

TABLE III. The axial dispersion coefficient in a two-phase RPC (correlations in the case of a G–L-system)

Systems and operating parameters	Correlation	Reference
Water (c) ↓ and air (d)↑; $D_c = 3.2$ and 5.4 cm; $f = 0.4 - 3$ Hz; $A = 0 - 1.5$ cm; $U_c = 0.05 - 0.58$ cm/s; $U_d = 0.044$ cm/s	$D_L = 1.7544 \cdot f \cdot h^{0.67} \cdot d \cdot D_c^{-0.67} \cdot \varepsilon^{-1.0}$	Miyauchi and Oya (1965)[17]
Water (c) ↓ and air (d) ↑; $D_c = 2.54$ cm; $f = 0.5 - 6.18$ Hz; $A = 0.65 - 1.5$ cm; $U_c = 0.38 - 1.2$ cm/s; $U_d = 0.8 - 3.2$ cm/s	$D_L = 90.5 \cdot U_R^{-0.964}$, $D_L = 81.47 \cdot U_L^{0.627} U_R^{-0.75 + 0.19} U_L$ where: $U_R = \dfrac{U_G}{\varepsilon_G} + \dfrac{U_L}{1-\varepsilon_G} + 2Af$	Skala (1980)[18]

TABLE IV. The axial dispersion coefficient in a two-phase RPC (correlations in the case of L–L-system)

Systems and operating parameters	Correlation	Reference
Single phase – water; and two phase; water (c)↑ and glycerin (d)↓; $D_c = 5.16$ cm; $f = 6.6 - 10$ Hz; $A < 0.4$ cm; $U_c = 0.28 - 1.5$ cm/s; $U_d = 0 - 0.5$ cm/s.	$f_{ef} = \left\{ \left[\left(1+\dfrac{1}{f}\right) \exp\left[6.6(h-4.5)\dfrac{\varepsilon^{2/3}U_c}{d\,A\,f} \right] -1 \right] \right\}^{-1}$ where: $f = \dfrac{\varphi}{\pi} - \dfrac{1}{2} - 2\dfrac{Af}{\pi}\cos\varphi = \arcsin\left(\dfrac{U_c}{2\pi Af}\right)$	Novetny et al. (1970)[19]
Water (c) ↑ and trichloroethylene (d) ↓; $D_c = 5$ cm; $f = 0.4 - 10$ Hz; $A = 0.15 - 0.45$ cm; $U_c = 0.3 - 0.5$ cm/s; $U_d = 0 - 0.45$ cm/s.	$D_{L2} = D_{L1} + \Delta D$ where: $\Delta D = 55 (h - 2m_2) d_{32}^{3}$; $2Af/\varepsilon^{0.66} < 6$; MS regime $\Delta D = 55 (h - 2m_2) d_{32}^{3} - 0.3$; $6 \leq 2Af/\varepsilon^{0.66} \leq 13$, D regime $\Delta D = 0.40\,\varepsilon_D/\varepsilon^{1.2} - 1.01$; $13 \leq 2Af/\varepsilon^{0.66}$, E regime 1.00 for $2Af/\varepsilon < 13.0$ $2m_2 = \begin{cases} 0.21 \cdot 2Af/\varepsilon & \text{for } 2Af/\varepsilon \leq 13.0 \text{ and } 2m_2 < 0.54 (h + 3.60) \\ 0.54 (h + 3.60) & \text{for other } \sqrt{\text{values}} \end{cases}$	Nemecek and Prochazka (1974)[10]
Water (c) ↓ and kerosene (d) ↑; $D_c = 5.08$ cm; $f = 0.5 - 6$ Hz; $A < 2.35$ cm; $U_c = 0 - 1.2$ cm/s; $U_d = 0 - 0.7$ cm/s.	$D_L = 5.62 \cdot A^{1.41} f^{0.73} h^{-0.88}$	Kim and Bairoi (1976)[11]

TABLE IV. Continued

Systems and operating parameters	Correlation	Reference
n-heptane (c) ↑ and water (d) ↓; $D_c = 2.54$ and 50.8 cm; $f < 6$ Hz; $A = 2.54$ cm; $U_c < 1.133$ cm/s; $U_d < 0.57$ cm/s	$D_{ds} = D_d \left(\dfrac{U_d}{u_d} \right) D_d \varepsilon$ D_{ds} – axial dispersion coefficient determined from the superficial velocity of the dispersed phase; D_d – axial dispersion coefficient of the dispersed phase $where$: $u_d = U_d/\varepsilon$ is the real velocity of the dispersed phase; The axial dispersion coefficient was determined only for the dispersed phase	Karr et $al.$ (1987)[20]

c – Continuous phase; d – dispersed phase; MS – mixer-settler regime; D – dispersion regime; E – emulsion regime.

TABLE V. The axial dispersion coefficient in a bubble column

Systems and operating parameters	Correlation	Reference
Water, acetone, CCl_4, ethanol, cyclohexanol, water solution of ethanol and sucrose (c) ↑ and N_2 (d) ↑; $D_C = 1.91$ and 4.57 cm; $U_L = 0.2 - 0.87$ cm/s; $U_G = 0.51 - 17.3$ cm/s.	$D_L = 0.344 U_G^{0.32} \rho_L^{0.07}$	Cova (1974)[21]
Water (c) (as a charge) and air (d) ↑; $D_C = 4$ and 8 cm; $U_G = 0 - 7$ cm/s.	$D_L = 0.3 U_G^{1.2} D_C^2 + 170 d^2$	Ohki and Inoue (1970)[22]
Water (c) (as a charge) and air (d) ↑; $D_C = 4$ and 8 cm; $U_G = > 10$ cm/s.	$D_L = 0.14 D_C/(1-\varepsilon_G)$	Ohki and Inoue (1970)[22]
Water (c) ↑ and air (d) ↑; $D_C = 6.6$ and 12.2 cm; $U_L = 0.5 - 1.5$ cm/s; $U_G = 0.30$ cm/s.	$\dfrac{U_G D_C}{D_L} = \dfrac{13 Fr_G}{1 + 6.5 Fr_G^{0.8}}$ where $Fr_G = U_G/\sqrt{g D_C}$	Kato and Nishiwaki (1971)[23]

TABLE VI. The axial dispersion coefficient in a packed-bed

Systems and operating parameters	Correlation	Reference
Water (k) ↓ and air (d) ↑; $D_c = 5.1$ cm; packing: Rashig rings 0.635 cm	$Pe_L = 1.00 \cdot Re_L^{0.70} Ga_L^{-0.32}$ where: $Pe_L = U_L d_p / D_L$; $Re_L = d_\pi \rho_L U_L / \mu_L$ and $Ga_L = d_p^3 g \rho_L^2 / \mu_L^2$	Michell and Furzer (1972)[24]

EXPERIMENTAL

The RPC consisted of a Pyrex tube equipped at the top and bottom with positions for the inlet and outlet of the liquid and gas phase. It could be operated in the counter-current mode (L – the liquid phase flow from the top to the bottom of the column and G – gas phase in the opposite direction), while the solid phase was used as a charge in the column. The vibration frequency of the perforated plate set was adjusted by a reduction control device and measured using an inductance counter.

A scheme of the experimental set-up in the case of a column of 2.54 cm i.d., as well as the plate characteristics (dimensions) are shown in Fig. 1, while the geometrical characteristics of the RPC used in this study and the operating parameters are given in Table VII.

TABLE VII. RPC geometry and operating parameters

Diameter (i.d)/cm	2.54
Height (column)/cm	207
Height of the working part of the RPC/cm	183.6
Vibration set length/cm	172.3
Volume of the column (working part)/cm³	839.3
Nozzle diameter (gas inlet)/cm	0.385
Rod diameter of the vibration set/cm	0.32
Number of plates	65
Plate diameter/cm	2.5
Distance between two plates/cm	2.54
Plate thickness/mm	1.5
Plate hole diameter/mm	8; 6
Number of holes on the plate	4 (8 mm) and 4/2 (6 mm)
Plate free area/%	51
Vibration amplitude/cm	2.35; 1.0
Vibration frequency/s⁻¹	2 – 4.5
Superficial gas velocity/cm/s	0 – 1.48
Superficial liquid velocity/cm/s	0.24 – 0.87
Solid phase content/%	0 and 5.61
Diameter of the solid spheres/mm	8.3
Plate (material)	s.s.
Distance between two plates	Teflon
Spheres (solid phase)	Polypropylene

The stimulus-response method based on tracer usage was applied for the determination of the residence time distribution function. An aqueous solution of tracer (sorbic acid; 2,4-hexadienoic acid; Industrie Betreuung-Belieferung, Gold-Schuidz, Austria). The tracer was injected into the liquid phase (water) at the column inlet (liquid phase) with the rate of injection presented in the form of a Dirac function (delta signal), and the response of such a signal was measured at the column outlet. In such a way the E – function (density of the residence time distribution function or external age distribution function) was determined and further processed with the goal of determining the Peclet number (Pe) and axial dispersion coefficient (D_L).

One part of the liquid at the outlet of the RPC was transferred to the quartz cell of a UV detector (LKB 2138 UVICORD S) with a peristaltic pump (LKB 2132 Micro Perpex Pump) for continuous measurement of the concentration of sorbic acid at 254 nm. The obtained data was continuously recorded (LKB 2210 Potentiometric Recorder). The quartz cell 2138-100 had a volume of 70 μl, with a light path of 5 mm.

Air from a compressor (4 bar) was used as the gas phase and introduced at the bottom of the column through a corresponding nozzle at a constant pressure of 170 kPa using an adequate pressure regulator. The
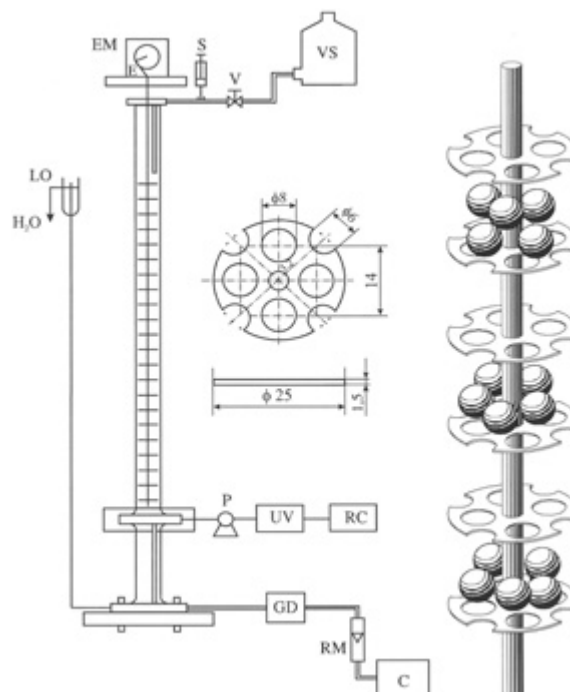

Fig. 1. Scheme of the experimental set-up (column diameter, i.d. = 25.4 mm), the solid phase arrangement and the dimensions of one plate mounted on the vibration set. Legend: C – compressor; E – excenter; EM – electromotor; GD – gas distributor; LO – liquid outlet; P – pump: RC – recorder; RM – rotameter; S – syringe; UV – detector; V – valve; VS – vessel for the liquid phase.

gas flow rate was adjusted by a valve and measured by a rotameter (VEB Prüfgeräte-Werk Mechanik Medingen). A specieal procedure and device was used to avoid flooding of the column at the beginning of gas flow. This device is a valve operating in the on-off regime for a few seconds, but only at the beginning of gas flow at the column bottom. After that period the valve was continuously open.

Tap water was used as the liquid phase. It was transferred from a reservoir 70 cm above the column into the RPC. The level in this tank was kept constant, so the pressure of the inlet water stream was always constant allowing a precise flow rate of the liquid phase.

Polypropylene spheres (density 890 kg/m^3 and diameter 8.3 mm) were used as the solid phase in the

RPC. The content of PP spheres was 5.61 % (calculated to the column volume), and their distribution was ordered (5 spheres were placed in every second space between two adjacent plates, Fig. 1).

RESULTS AND DISCUSSION

The determined axial dispersion coefficient in the case of one phase (L) flow ranged from 0.81 to 5.79 cm^2/s, for the two phase G–L system from 1.61 to 6.47 cm^2/s, and for the two phase L–S system from 1.55 to 14.12 cm^2/s, and for the three phase G–L–S system from 1.19 to 8.58 cm^2/s. The obtained data for the G–L system were almost identical to some previously published in the literature which ranged from 2.31 to 7.61 cm^2/s for $U_G = 0.80 – 3.13$ cm/s, $Af = 0.66–9.17$ cm/s, and for counter-current flow of the gas (air) and liquid phase (the same type of column with 65 plates, $i.e.$, 64 sections between the plates; i.d. 2.54 cm).[18]

Only a negligible influence of the continuous phase flow rate (water) on the axial dispersion was determined in one (L) and two phase (G–L) systems as indicated in Fig. 2 and also mentioned in some other investigations.[25] A slightly greater influence of the liquid flow rate was detected in two (L–S) and three phase systems (G–L–S). By introducing the solid phase as a charge into the RPC, which was regularly distributed along the column height, $i.e.$, in the axial direction, the mixing of phases (L or G and L) inside the column became more intensive and, consequently, the axial dispersion increased. There are only a few data concerning the influence of the solid phase on mixing and axial dispersion in the literature.[26,27] In this investigation one can imagine that the PP spheres had a similar influence on liquid flow as do gas bubbles. The effects of channelling and recycling of the liquid around the solid spheres is based on the same mechanism as those around gas bubbles, the only difference being that the dispersion (disintegration) of solid spheres can not be improved with a higher vibration intensity as is possible in the case of gas bubbles. The difference between the densities of the liquid phase and PP spheres (1000 and 930 kg/m^3, respectively) was much smaller compared to the same difference between the liquid and gas phase. A very small probability of PP sphere accumulation just below the plate exists in the case of those spheres placed in a space between two plates that is usually observed in a G–L system at a lower vibration intensity (the so called M–S regime of column operation). On the other hand, the diameter of the PP sphere (8.3 mm) is larger than the hole diameter of the plate (8 mm), so physically it is impossible for the spheres to be transferred from one to the other interplate space (Fig. 1).

An additional effect of the gas, solid or both phases together on liquid phase mixing in the RPC is presented in Fig. 3. As may be seen from the calculated dispersion coefficient, at smaller vibration intensity (Fig. 3a), the increase of axial mixing caused by the presence of the solid phase (PP spheres) in the RPC is smaller than those induced by the presence of a gas phase. Furthermore, the effect of gas superficial velocity on axial mixing (D_L) decreases with increasing vibration intensity (Fig. 3b). Data on the axial dispersion were gathered at a vibration intensity of $I = 7.05$ cm/s and could be divided into the following ranges: D_L increases in the L–S system in the presence of the solid phase (1.8 to 2.58 times larger), and for the G–L–S system (1.6 to 1.8 times larger) compared to the D_L value for a one phase (L) system. Moreover, for the same I value, the ratio of axial dispersion in G–L
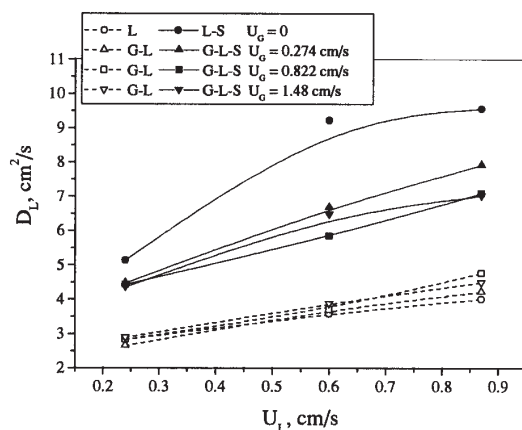
Fig. 2. The dependence of the axial dispersion of the liquid phase in a RPC on the superficial liquid velocity ($A = 2.35$ cm, $f = 3$ Hz).

and L systems is about 1 (Fig. 3c). Axial dispersion seems to be more pronounced for the L–S, somewhat smaller for the G–L–S and negligibbe for the G–L system. On further increasing the vibration intensity to values greater than 9.4 cm/s, the axial dispersion in the G–L–S, as well as in the G–L, becomes equal to the values of D_L in the case of a one (L) phase system, the ratio of these axial dispersions being in the range of 0.7 and 1.2. Only in the case of the L–S system, does liquid back mixing, expressed in the form of the D_L – coefficient of axial dispersion, deviate to a larger extent from the corresponding value for a one phase system (1.6 to 2.4 times – Fig. 3d). Increased vibration causes uniformity and better gas bubble dispersion in the liquid phase and, consequently, axial mixing in the G–L as well as in the G–L–S RPC are almost the same. Figs. 3a and 3d confirm that a complex interference probably exists between the vortex created by the mixing device (vibration of the perforated plate set) and those caused by the liquid flow.

The relations between the axial mixing and superficial gas velocity U_G in the case of two (G–L) and three phase (G–L–S) RPCs are given in Fig. 4. Axial dispersion increases (G–L system) with increasing gas flow rate for the smallest vibration intensity ($I = 2$ cm/s, Fig. 4a), as well as for a 2 times higher vibration intensity ($I = 4$ cm/s, Fig. 4b). However, at $I = 7.05$ cm/s (Fig. 4c) there is no evidence that the superficial gas velocity influences the axial dispersion of the liquid phase in the G–L system, while the axial dispersion decreases in the G–L–S system. At the largest vibration intensity, $I = 9.4$ cm/s (Fig. 4d), the decreasing tendency of the axial mixing is accompanied by an increasing superficial gas velocity in the case of the G–L system. For the three phase system (G–L–S), a decrease of D_L is evident up to a certain values of U_G (the existence of a minimum at $U_G = 0.5$ cm/s) and then back-mixing of the liquid phase starts to slightly increase again.

Gas bubbles cause the main mixing of the liquid phase for the G–L system in the case of the lowest vibration intensity. The up-flow of gas bubbles through the holes of the perforated plates is the main reason for the back-mixing of the liquid phase in this regime of col-
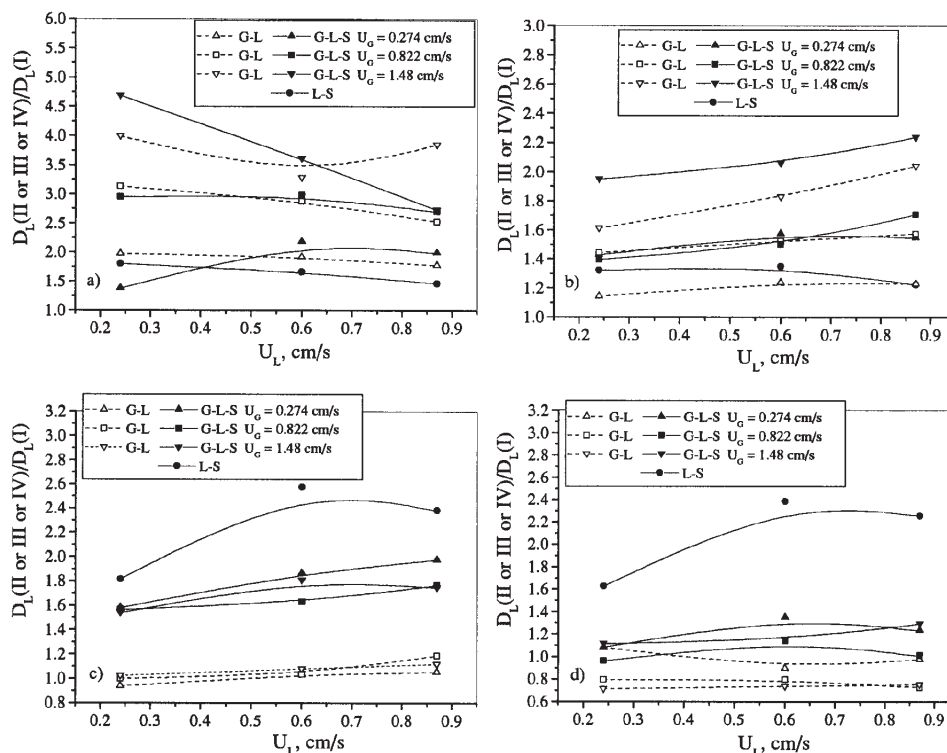
Fig. 3. The relative ratio of the axial dispersion of the liquid phase in the RPC in the case of two and three phase systems (G–L; L–S; G–L–S) and a one (L) phase system as a function of the superficial liquid velocity: a) $A = 1$ cm, $f = 2$ Hz, b) $A = 1$ cm, $f = 4$ Hz, c) $A = 2.35$ cm, $f = 3$ Hz, d) $A = 2.35$ cm, $f = 4$ Hz.

umn operation compared to the effect of mixing initiated by the vibration stirrer. However, at the largest vibration intensity ($I = Af$), the bubble dispersion slightly decreases (Fig. 4; $I = 9.4$ cm/s) with increasing superficial gas velocity. The reduction of D_L at the highest U_G might be caused by a reduced effect of liquid circulation and the formation of many small bubbles in each interplate space when the column operates in an emulsion regime. Other effects, such as the accumulation of gas bubbles under the plates are less probable with the large open area of the plates used in this study (51 %). The same conclusions that D_L increases with increasing U_G at lower vibration intensities, almost independent of the vibration in the case of moderate intensities, and that D_L decreases in the case of larger gas flow rates and high vibration intensities have been drawn in other investigations of axial mixing in a RPC of the following geometry and operating conditions[11]: $D_C = 5.08$ cm; $L = 1.8$ m; $h = 2.7$ cm, d = 6.35 and 12.7 and 14.3 mm; $\varepsilon = 0.49$; $A = 1.1$ and 1.55 cm; $f = 0.5$ and 1 Hz; $U_L = 0 - 0.27$ cm/s; $U_G = 0 - 0.7$ cm/s.

Such behavior might be explained by the formation of a liquid vortex, its movement and, finally, its disappearance. At lower vibration intensities in the L–S system there is a small number of vortexes and, also, the size of the individual vortexes is small because only a limited number of solid spheres are present in the RPC. By introducing the gas
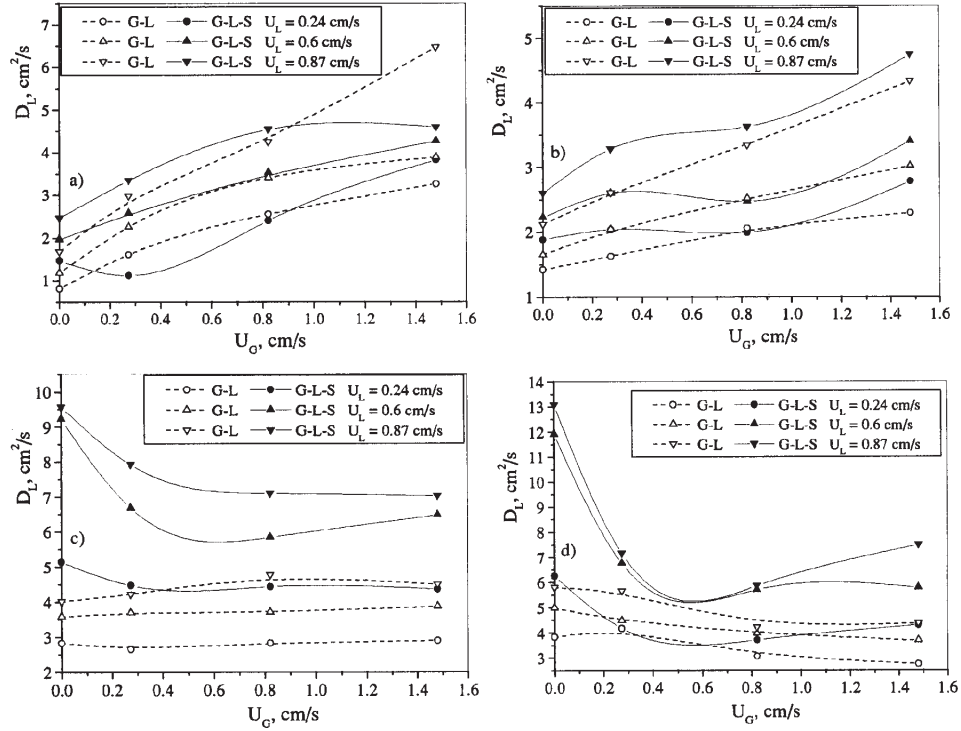
Fig. 4. Relation between the axial dispersion and the superficial gas velocity for G–L and G–L–S systems in a RPC: a) $A = 1$ cm, $f = 2$ Hz, b) $A = 1$ cm, $f = 4$ Hz, c) $A = 2.35$ cm, $f = 3$ Hz, d) $A = 2.35$ cm, $f = 4$ Hz.

phase in the RPC, thus making a three phase G–L–S system, the number of smaller-sized bubbles increases as does the number of liquid vortexes. These vortexes are formed in the simultaneous movement of plates, bubbles and solid particle. As the number of solid spheres in the RPC in the case of L–S and G–L–S system is the same, the number of vortexes increases only as a consequence of the larger number of bubbles. It is then to be expected that the presence of gas in the RPC increases liquid mixing, *i.e.*, axial dispersion. On the other hand, in the case of the L–S system, increasing the vibration intensity in the absence of gas bubbles causes the formation of a larger vortex thus causing greater axial mixing. However, in the presence of the gas phase, a large number of small bubbles is created which are formed by the disintegration of larger bubbles in contact with the plates and solid spheres thus depressing the liquid circulation in the column. The vortex lifetime is decreased by gas bubbles passing through it. Simultaneously bubbles also influence the creation of vortexes, meaning that many smaller vortexes can probably be formed and they can move in all directions. These different mechanisms of vortex formation and interference again decrease the vortex lifetime and, consequently decrease the axial mixing effect.

However, it must be pointed out that the change in vibration intensity, defined simply as the product of the amplitude (*A*) and frequency (*f*) of vibration ($I = A \cdot f$), as shown in Fig. 4, was caused by changing both operating parameters (*A* and *f*). It has previously been re-
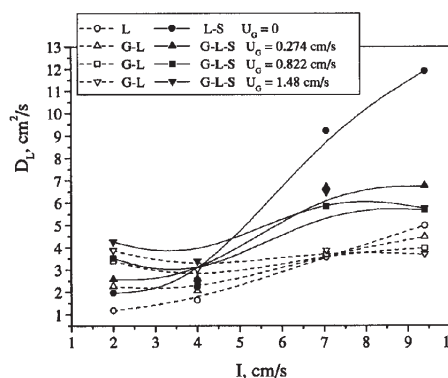
Fig. 5. Dependence of axial mixing on the vibration intensity: $U_L = 0.6$ cm/s, $D_c = 2.54$ cm, $\varepsilon_S = 0$ (L and G–L); $\varepsilon_S = 5.61$ % (L–S and G–L–S).

ported[28–30] that the amplitude has a negligible effect on axial mixing in the case of single and a more expressed influence in two phase RPCs. During dispersion mixing in a RPC, in the case of this investigation characterized by a distance between two plates of 2.54 cm, and 1 cm amplitude, there is one small zone of relatively low mixing inside this space which the plates do not reach at all (plate movement from the maximum to minimum position, *i.e.*, 2*A*). Stevens and Baird[14] defined this space inside one compartment of a RPC (*i.e.*, the distance between two adjunct plates) as a region of "pure" mixing as opposed to the other part of one compartment which was designated as the "well" mixed zone. The pure mixing region is represented by a relatively small volume of column space (0.5 cm length) in the case of a 2.54 cm compartment (distance between two plates) and $A = 1$ cm, which can also be mixed well by vortex movement. In the other case presented in Fig. 4, where $A = 2.35$ cm, the distance of the space with good mixing behavior (2*A*) is 4.7 cm with an overlapping zone of two adjacent compartments of more than 2 cm. These regions are, according to the above analysis, mixed two times better compared to the other zones in the RPC. The optimal distribution between the plate distance (*h*) and amplitude of vibration (*A*) the case when a "pure" mixed region does not exist would be $h = 2A$.

The dependence of axial mixing on the vibration intensity for one-, two- and three- phase systems is presented in Fig. 5. Generally, axial mixing (D_L) is more expressed in the presence of the solid phase (L–S and G–L–S systems), and also for systems without gas flow (aeration).

The relative increase of axial mixing is shown in Figs. 6 for G–L (6a), L–S (6b) and G–L–S systems (6c) compared to the axial mixing of a single phase RPC (L only). The presence of the gas phase increases back-mixing of the liquid phase 0.75 to 4 times (Fig. 6a), the solid phase 1.25 to 2.75 times (Fig. 6b), and both of these phases together (Fig. 6c) 1 to 4.75 times. The ratio of axial mixing in systems which include a gas phase (G–L and G–L–S) and the one phase system (L) decreases with increasing vibration intensity. In a RPC without aeration (L–S), this ratio is variable and higher for intensive mixing (larger vibration intensity). For the G–L system this ratio is almost 1 for $I > 7$ cm/s.

The obtained results indicate that axial mixing depends on the vibration intensity, the
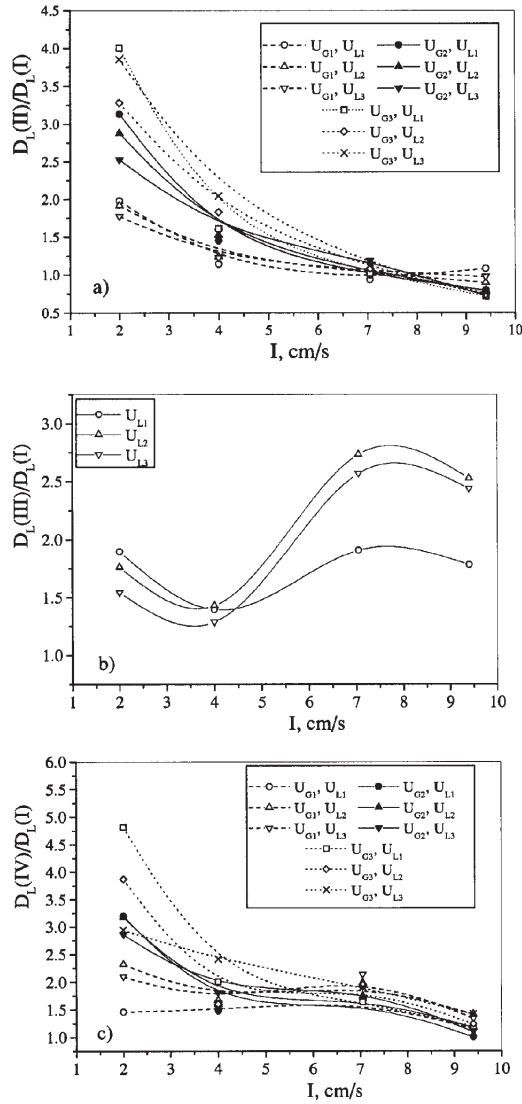
Fig. 6. The ratio of axial mixing of a two-phase RPC (a: G–L; and b: L–S) and a one phase RPC (L only) and the same ratio of a three-phase RPC (c: G–L–S) and a one phase RPC (L); $U_{L1} = 0.24$; $U_{L2} = 0.6$; $U_{L3} = 0.87$; $U_{G1} = 0.274$; $U_{G2} = 0.822$; $U_{G3} = 1.48$ cm/s.

superficial gas and liquid velocity, column diameter and content of solid phase in the column. In the case of a one phase liquid system (L only), the following correlation between the operating parameters and the axial mixing coeffcient was derived by applying statistical analysis:

$$D_L = 0.49(Af)^{1.11} U_L^{0.31} \qquad (4)$$

The difference between the value calculated according to equation 4 and the experimentally determined value of the dispersion coefficient is ± 15.5 %. The same type of cor-

relation was derived for all the other investigated systems as follows.

G–L system:

$$D_L = 3.37(Af)^{0.17} U_L^{0.31} U_G^{0.07} \qquad \pm 20.6\,\% \tag{5}$$

L–S system:

$$D_L = 1.26(Af)^{1.42} U_L^{0.51} \varepsilon_s^{0.23} \qquad \pm 32.5\,\% \tag{6}$$

G–L–S system:

$$D_L = 1.39(Af)^{0.47} \cdot U_L^{0.42} U_G^{0.03} \varepsilon_s^{-0.26} \qquad \pm 28.6\,\% \tag{7}$$

All of the above correlations may be applied only in the cases of reciprocating plate vibration ($I > 0$).

For $I = 0$ another type of correlation was tested by using the ratio of the Peclet number (as the y-axis, Pe^{-1}) and the product of the Reynolds and Schmidt number (defined on the x-axis). In a log-log plot such a correlation showed linear dependence with a small difference between the calculated and experimentally determined values of axial mixing. Such a correlation was also tested for some other data published in the literature (Fig. 7).
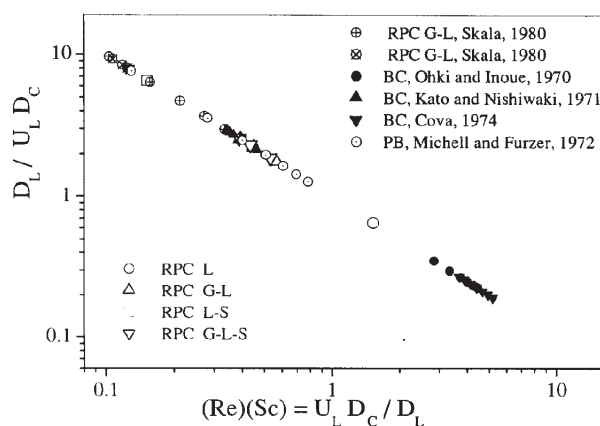

Fig. 7. Dispersion number (Pe^{-1}) of the RPC related to the product of the Reynolds and Schmidt number ($Re \cdot Sc$) for the case of $I = 0$ cm/s.

According to the values of the axial dispersion coefficient measured in the RPC and those values determined in other types of columns (bubble column and packed bed), it can be concluded that the much smaller back mixing in a RPC favorizes a specific type of heterogeneous catalyzed reaction between the gas and liquid phase. A brief schematic overview of the mixing effect is presented in Figs. 8 and 9.

CONCLUSIONS

Good agreement between the determined axial dispersion coefficient in a RPC and that published in the literature for the same column geometry and similar operating parameters was obtained for one phase (L–liquid only) and two-phase systems (G–gas and L–liquid phase counter-current flow). New data on the axial mixing effect are presented for a three-phase RPC system.
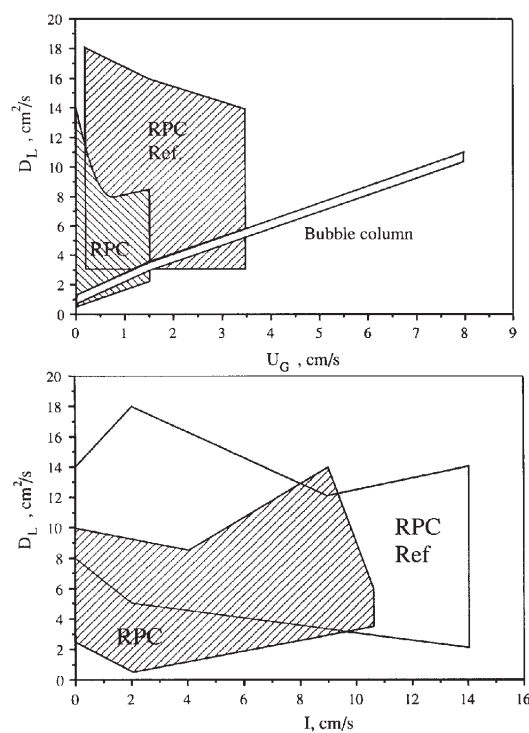
Fig. 8. Influence of the superficial gas velocity and vibration intensity on the axial mixing in the RPC (this study) and data from the literature for the same type of column (RPC ref. – Miyauchi and Oya[17]; Skala[18]) and influence of the superficial gas velocity on the axial mixing in a bubble column (Cova[21]; Ohki and Inoue[22]; Kato and Nishiwaki[23]).
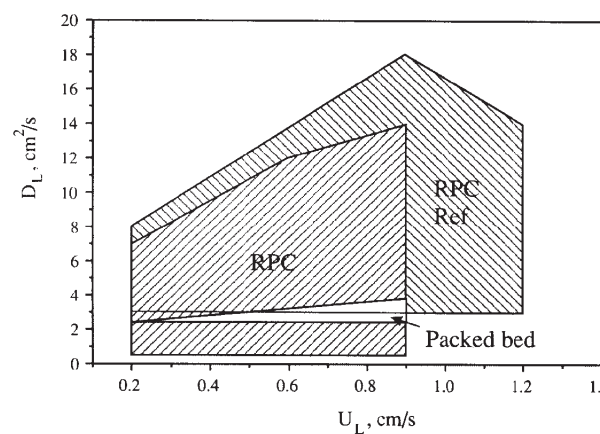

Fig. 9. Influence of the superficial liquid velocity on the axial mixing in the RPC (this study) and data from the literature for the same type of column (RPC ref. – Miyauchi and Oya[17]; Skala[18]) and for a packed-bed column (Michell and Furzer[24]).

The presences of the gas-phase in a RPC increases the axial mixing, which is more expressed at higher gas and liquid (counter-current flow) superficial velocities. Gas bubbles influence channelling and liquid recycling, which means a higher degree of axial mixing.

The additional effect of the solid phase on axial mixing is smaller compared to the ad-

ditional effect of the gas phase for smaller vibration intensities. The largest increase of axial mixing occurs in aerated two- and three-phase systems at lower vibration intensities. An almost identical effect of mixing exists in the case of the L, G–L and G–L–S systems. A larger deviation was observed only for the L–S system.

The presence of a solid phase in the RPC increases axial mixing to a smaller extent at lower vibration intensities, low liquid flow rate and at higher vibration intensities. Such an effect is very important in the case of RPC usage as a bioreactor where axial mixing inside a column could be adjusted to a value enabling the highest reactor productivity.

In the presence of the gas phase, axial mixing of the liquid phase depends mostly on the presence of bubbles and their movement (lower vibration intensity). However, at higher vibration intensities many smaller bubbles are created, which have the tendency of decreasing the lifetime of the vortexes in the liquid phase, thus leading to lower axial dispersion of the L phase. Comaparison between L and G–L, as well as between L–S and G–L–S systems (*i.e.*, systems without and with aeration) indicate that in the cases of the aerated systems, the vibration intensity has a smaller effect on axial dispersion. The corresponding dependencies of axial dispersion and vibration intensity indicate the existence of a similar mechanism (curve type) and the value of the dispersion coefficient is only higher in the presence of a solid phase.

The correlations for determining the axial dispersion coefficient was derived for the different systems used in this study, of which the more important ones are for L–S and G–L–S systems.

SYMBOLS

A	– Amplitude of vibration, cm
C	– Concentration of tracer, mol/dm^3
D_L	– Axial dispersion coefficient, cm^2/s
$D_L(I)$	– Axial dispersion coefficient one phase system (L), cm^2/s
$D_L(II)$	– Axial dispersion coefficient two-phase system (G–L), cm^2/s
$D_L(III)$	– Axial dispersion coefficient two-phase system (L–S), cm^2/s
$D_L(IV)$	– Axial dispersion coefficient three-phase system (G–L–S), cm^2/s
D_c	– Column diameter, cm
d	– Plate hole diameter, mm
d_p	– Characteristics of the column package, cm
E_t	– External age distribution function, min^{-1}
h	– Distance between two adjunct plates, cm
f	– Frequency of vibration, Hz
I	– Intensity of vibration, $I = Af$, cm/s
L	– Column height (operating part), cm
I_b	– Mixing length caused by the force of surface tension, cm
I_m	– Mixing length caused by mechanical mixing, cm
Pe	– Peclet number
q	– Back flow through the perforated plate
t	– Time, min
U_c	– Superficial velocity (continuous phase), cm/s

U_d – Superficial velocity (dispersed phase), cm/s
U_G – Superficial velocity (gas phase), cm/s
U_L – Superficial velocity (liquid phase), cm/s
V – Volume of the column, cm^3

Greek symbols

δ – Plate thickness, mm
ε – Ratio of free area of the plate
ε_S – Volume fraction of the solid phase in the dispersion
ε_G – Volume fraction of the gas phase in the dispersion
ε_D – Volume fraction of the dispersed phase
ε_b – Dissipated energy in the process of overcoming surface tension, W/kg or cm^2/s^3
ε_t – Totally dissipated energy, W/kg or cm^2/s^3
μ_L – Viscosity, Pa s
ρ_1 – Liquid phase density, kg/m^3
υ – Gas flow rate, cm^3/s

ИЗВОД

АКСИЈАЛНО МЕШАЊЕ ТЕЧНЕ ФАЗЕ У ТРОФАЗНОЈ КАРОВОЈ КОЛОНИ СА ВИБРАЦИОНОМ МЕШАЛИЦОМ

ЉУБИША Б. НИКОЛИЋ[1], ВЕСНА Д. НИКОЛИЋ[1], ВЛАДА Б. ВЕЉКОВИЋ[1], МИОДРАГ Л. ЛАЗИЋ[1] и ДЕЈАН У. СКАЛА[2]

[1]Технолошки факулшеш, Булевар ослобођења 124, 16000 Лесковац и [2]Технолошко-мешалуршки факулшеш, Карнеђијева 4, 11000 Београд

Испитиван је утицај интензитета вибрације и протока гаса на аксијалну дисперзију течне фазе у присуству сферних честица полипропилена које су као шаржа чврсте фазе унете по одређеном распореду у Карову колону (колона са вибрационом мешалицом). Одређивање коефицијента аксијалне дисперзије течне фазе засновано је на примени методе побуде и одзива тј. на бази експериментално одређене функције густине расподеле времена задржавања течности у колони. Водени раствор сорбинске киселине, који је у облику импулсног сигнала додаван у течност која притиче у колону, употребљен је као обележени део флуида (трасер), а спектрофотометријски измерена концентрација сорбинске киселине на излазу из колоне са вибрационом мешалицом је била основ за одређивање функције густине расподеле времена задржавања (Е–функције). Анализом експериментално одређене Е–функције и оне која важи за модел струјања у коме постоји аксијално мешање течне фазе израчунаван је коефицијент аксијалне дисперзије течне фазе. Овако измерени и израчунати подаци о струјању течности у колони искоришћени су у циљу извођења одговарајућих корелационих зависности које могу успешно да се примене за предсказивање коефицијента аксијалне дисперзије у колони са вибрационом мешалицом типа Кар, унутрашњег пречника 2,54 cm. Ове корелације повезују коефицијент аксијалне дисперзије, проток гаса и течне фазе и интензитет вибрације за двофазни систем гас-течност, односно проток течне фазе, садржај чврсте фазе и интензитет вибрације за систем течност-чврста фаза, и протока гаса и течне фазе, интензитета вибрације и удела сферних честица полипропилена у колони у случају анализе струјања течне фазе у трофазном систему гас–течност–чврста фаза у овој колони.

(Примљено 27. маја 2003, ревидирано 2. фебруара 2004)

REFERENCES

1. W. J. D. Van Dijck, US Patent 2.011.186 (1935)

2. A. E. Karr, *AIChE J.* **5** (1959) 446

3. M. H. I. Baird, N. V. Rama Rao, *Can. J. Chem. Eng.* **76** (1998) 370

4. H. Brauer, *Bioprocess Eng.* **6** (1991) 1

5. J. Audet, M. Lounes, J. Thibault, *Bioprocess Eng.* **15** (1996) 209

6. J. Audet, J. Thibault, A. LeDuy, *Biotechnol. Bioeng.* **52** (1996) 507

7. J. Audet, H. Gagnon, M. Lounes, J. Thibault, *Bioprocess Eng.* **19** (1998) 45

8. H. Gagnon, J. Thibault, F. Cormier, C. B. Do, *Bioprocess Eng.* **21** (1999) 405

9. D. Skala, J. Mićić, *Hem. Ind.* **36** (1982) 136

10. M. Nemecek, J. Prochazka, *Can. J. Chem. Eng.* **52** (1974) 739

11. S. D. Kim, M. H. I. Baird, *Can. J. Chem. Eng.* **54** (1976) 81

12. S. D. Kim, M. H. I. Baird, *Can. J. Chem. Eng.* **54** (1976) 235

13. D. Skala, *M. Sc. Thesis*, Faculty of Technology and Metallurgy, University of Belgrade, Belgrade, 1976

14. G. W. Stevens, M. H. I. Baird, *Chem. Engng. Sci.* **45** (1990) 457

15. M. H. I. Baird, N. V. Rama Rao, *AIChE J.* **37** (1991) 1019

16. M. H. I. Baird, N. V. Rama Rao, S. Vijayan, *Can. J. Chem. Eng.* **70** (1992) 69

17. T. Miyauchi, H. Oya, *AIChE J.* **11** (1965) 395

18. D. Skala, *Ph. D. Thesis*, University of Belgrade, Belgrade, 1980

19. P. Novotny, J. Prochazka, J. Landau, *Can. J. Chem. Eng.* **48** (1970) 405

20. A. E. Karr, S. Ramanujam, T. C. Lo, M. H. I. Baird, *Can. J. Chem. Eng.* **65** (1987) 373

21. D. R. Cova, *Ind. Eng. Chem. Process Desing Develop.* **13** (1974) 292

22. Y. Ohki, H. Inoue, *Chem. Eng. Sci.* **25** (1970) 1

23. Y. Kato, A. Nishiwaki, *Kagaku Kogaku* **35** (1971) 912

24. R. W. Michell, I. A. Furzer, *Chem. Eng. J.* **4** (1972) 53

25. P. Parthasarathy, G. Sriniketan, N. S. Srinivas, Y. B. G. Varma, *Chem. Engng. Sci.* **39** (1984) 987

26. Lj. Nikolić, N. Đoković, V. Veljković, D. Skala, *Hem. Ind.* **53** (1999) 300

27. Lj. Nikolić, V. Veljković, D. Skala, *Chem. Ind.* **55** (2001) 249

28. M. H. I. Baird, N. V. Rama Rao, *Can. J. Chem. Eng.* **66** (1988) 222

29. M. Lounes, J. Thibault, *Can. J. Chem. Eng.* **74** (1996) 187

30. M. Lounes, J. Thibault, in *Mixed – Flow Hydrodynamics*, Nicholas P. Cheremisinoff Ed., Gulf Publishing Co., Houston, 1996, p. 457.